Second International Conference on CFD in the Minerals and Process Industries
CSIRO, Melbourne, Australia
6-8 December 1999

NUMERICAL SIMULATION OF ALUMINIUM METAL TAPPING

N.X. CHEN Y.J. XU

Institute of Engineering Thermophysics, CAS, P.O. Box 2706, Beijing 100080, CHINA

J.J.J. CHEN X.D. CHEN

Dept. of Chemical and Materials Engineering, The Auckland University, Private Bag 92019, Auckland, NEW ZEALAND

M.P. TAYLOR

Comalco Smelting, Brisbane, AUSTRALIA

Z.D. CHEN

Advanced Thermo-Fluids, Technologies Laboratory, CSIRO Building, Construction and Engineering, P.O. Box 56, Highett, Victoria 3190, AUSTRALIA

ABSTRACT

The removal of molten liquid aluminum metal from Hall-electrolytic cell in its production by electrolysis method is a "tapping" process. The electrolytic cell suffers localized wear of the cathode, which is near the entrance region of the tapping pipe, during this operation. It is evident that the phenomenon of cathode erosion is a mass transfer process. Because the intensity of mass transfer is a function of skin friction, or drag force per area, the intensity of cathode erosion is proportional to the surface stress and velocity in the entrance region on the cathode bottom. This hydrodynamics problem can be solved by computational fluid dynamics. The objective of the present paper is to simulate tapping flow and to study its features using Navier-Stokes solver with the view to improve this process and reduce the operation and production costs. The method applied here is based on a pressure correction technique and coupled with a two-equation turbulence model. A wall function is also used for reducing the number of meshes. The mesh used is a general structured body-fitted grid system where the curvilinear coordinate lines are coincided with the boundaries of the flow domain. As an example, a typical tapping flow field is calculated. The calculated results and the studies on the effects of the leaning angle and the clearance on the surface stress are also presented.

NOMENCLATURE

B	liquid (bath-metal) height
C_1, C_2, C_μ	empirical coefficients (see Eqs.(2),(5))
G	production rate of turbulent kinetic energy (see Eq.(6))
Hcl	clearance height
$\vec{i}_x, \vec{i}_y$	unit vectors along x- and y-coordinates
J	Jacobian , $J = \sqrt{g}$
P	total pressure and inlet total pressure
p	static pressure
p_b	static pressure at outlet from pipe
S_Φ	source term (see Eq.(3-5))
$S_i^{'}(x^1, x^2)$	source term (see Eq.(9))
t	time
V_{exit}	exit velocity from tapping pipe
$\vec{V}, V^j, V_j$	velocity vector and its physical contravariant and physical covariant components
V_x, V_y or v_x, v_y	x- and y-components of velocity vector
$V / V_{\sigma=90}$	relative value of velocity at the first point from bottom wall
$V_{\sigma=90}$	velocity at the first grid point from the bottom wall at inlet of clearance zone for $\sigma = 90^o$
ε	dissipation rate of turbulent energy
$\Phi = 1, v_x, v_y, \kappa, \varepsilon$	one of the variables to be solved,
$\Gamma_\Phi = 0, \mu_{eff}, \mu_{eff}, \mu_t / \sigma_\kappa, \mu_t / \sigma_\varepsilon$	one of the effective diffusion coefficients,
κ	turbulent kinetic energy
$\mu_l, \mu_t, \mu_{eff} (or \mu)$	laminar, turbulent and effective dynamic viscosity
ρ	density
σ	leaning angle of tapping pipe
τ	shear stress

INTRODUCTION

Metal produced in an aluminum electrolytic cell is removed by vacuum using a crucible and a tapping pipe. Serious localized cathode degradation occurs near the entrance region of the tapping pipe. In the operational cells the erosion mechanisms may conclude erosion-corrosion of aluminum carbide, dissolution of carbon (aluminum

carbide), direct abrasion of the carbon by molten metal, etc. The serious degradation may prolong the operation period and increase production cost. Because the intensity of mass transfer is a function of skin friction, or drag force per area, the intensity of cathode erosion is proportional to the surface stress and velocity in the entrance region on the cathode bottom. Therefore, the tapping problem can be simulated experimentally and numerically. Due to the rapid process of computer science technology and computational technique CFD can be used as a powerful tool to calculate and to understand the flow mechanisms, and then to improve the tapping conditions.

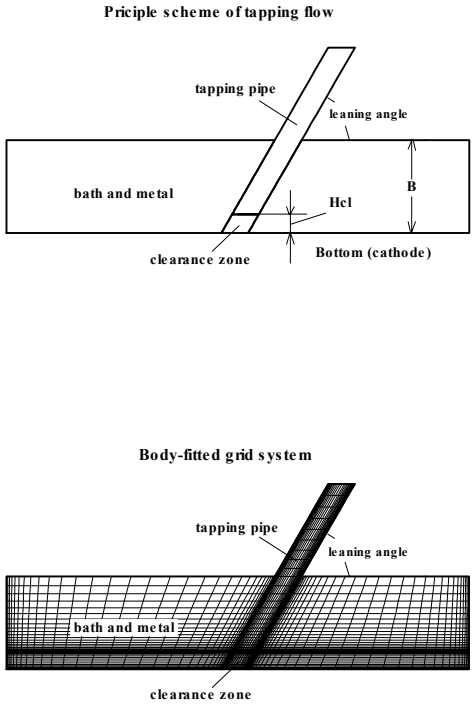

Figure 1. Principle scheme and body-fitted grid system.

The objective of this paper is to simulate tapping flow and to study its features using Navier-Stokes solver with the view to improve this process and then reduce the operation and production cost.

Firstly, the current method for the tapping flow calculation is presented. It is based on the Reynolds-averaged Navier-Stokes equations with a two-equation turbulence model and solved by a pressure correction method. The present method is derived from authors' previous method (Chen and Xu, 1990, 1991). The time-averaged Navier-Stokes equations are written in a generalized form. The unknown variables of the momentum equations are still two components of velocity vector expressed by Cartesian coordinate system. Using the pressure correction technique the algebraic discretized equations are solved. In this method a central volume approximation is used for all diffusion term, and an up-winding scheme is used for convection terms. The solutions of the algebraic discretized equations can be obtained by successive iterations with the linear relaxation method. Then, a two-dimensional typical tapping problem is solved. Here a non-uniform grid system is shown. Its coordinate lines are marched with the boundaries of the flow domain. As shown in this paper, finer meshes are adopted near the boundaries, walls and the tapping entrance region. From the process physics it is seen that the intensity of cathode erosion is proportional to the surface stress and velocity in the entrance region on the cathode bottom. The surface stress is influenced by the geometrical parameters, such as leaning angle of the tapping pipe, clearance value between the entrance to the pipe and the cathode bottom, the depth of liquid metal and the tapping spout form, etc. Due to the limitation of the paper the first two problems are only presented. The present numerical study gives us an orientation of improvement of these two parameters.

NUMERICAL METHOD

Governing equations expressed by Cartesian coordinate system

In the present paper the *x*- and y-components of the momentum equation are used, and then the variables of the momentum equation are v_x and v_y. The above-mentioned governing equations for steady flow coupled with $\kappa-\varepsilon$ model expressed by the Cartesian coordinate system can be written in a generalized form as follow:

$$\frac{\partial(\rho\Phi)}{\partial t}+\frac{\partial(\rho v_x\Phi)}{\partial x}+\frac{\partial(\rho v_y\Phi)}{\partial y}= \frac{\partial}{\partial x}(\Gamma_\Phi\frac{\partial\Phi}{\partial x})+\frac{\partial}{\partial y}(\Gamma_\Phi\frac{\partial\Phi}{\partial y})+S_\Phi \quad (1)$$

where: Φ denotes the variable to be solved, $\Phi=1,v_x,v_y,\kappa,\varepsilon$; Γ_Φ is the effective diffusion coefficient and S_Φ is the source term. They are defined as: $\Gamma_\Phi=0,\mu_{eff},\mu_{eff},\mu_t/\sigma_\kappa,\mu_t/\sigma_\varepsilon$ and $S_\Phi=0,S_{v_x},S_{v_y},S_\kappa,S_\varepsilon$ for continuity equation, two components of momentum equation, $\kappa-$ and $\varepsilon-$equations, respectively. The empirical coefficients are $\sigma_\kappa=1.0$ and $\sigma_\varepsilon=1.3$. The effective dynamic viscosity μ_{eff} can be determined as: $\mu_{eff}=\mu_t+\mu_t$. Later we will denote μ_{eff} by μ. The turbulent dynamic viscosity is calculated as follows:

$$\mu_t=C_\mu\rho\ \kappa^2/\varepsilon \quad (2)$$

The source terms can be calculated from the expressions:

$$S_{v_x}=\partial(\mu\partial v_x/\partial x)/\partial x+\partial(\mu\partial v_y/\partial x)/\partial y -(2/3)\partial(\mu div\vec{V})/\partial x-\partial p/\partial x \quad (3a)$$

$$S_{v_y}=\partial(\mu\partial v_x/\partial y)/\partial x+\partial(\mu\partial v_y/\partial y)/\partial y -(2/3)\partial(\mu div\vec{V})/\partial y-\partial p/\partial y \quad (3b)$$

$$S_\kappa=\mu_t G-\rho\varepsilon \quad (4)$$

$$S_\varepsilon=C_1\mu_t(\varepsilon/\kappa)G-C_2\rho\varepsilon^2/\kappa \quad (5)$$

where G is the production rate of turbulence kinetic

energy. It is calculated by the following formulas:

$$G = 2[(\partial v_x/\partial x)^2 + (\partial v_y/\partial y)^2] + (\partial v_x/\partial y + \partial v_y/\partial x)^2 \quad (6)$$

In Equations (2) and (5) C_1, C_2, C_μ are the empirical coefficients of $\kappa-\varepsilon$ model. They are 1.47, 1.92, 0.09, respectively.

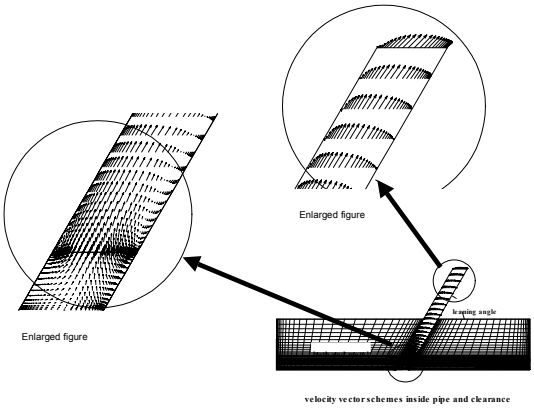

Figure 2. Velocity vector schemes inside pipe and clearance.

Governing equations expressed by body-fitted coordinate system

The mesh employed is a general structured grid system where curvilinear coordinate lines coincide with the boundaries of the flow domain. Therefore, it is needed to use the coordinate transformation technique to have a body-fitted coordinate system. Then, introducing new independent variables, $x^1 = x^1(x, y)$, $x^2 = x^2(x, y)$, the generalized form of the governing equations, Eq.(1), can be expressed by the body-fitted curvilinear coordinate system as follows:

$$\frac{\partial(\rho\sqrt{g}\Phi)}{\partial t} + \frac{\partial(\rho V^1\Phi)}{\partial x^1} + \frac{\partial(\rho V^2\Phi)}{\partial x^2} = \frac{\partial(J\Gamma_\Phi g^{11}\dfrac{\partial\Phi}{\partial x^1})}{\partial x^1} + \frac{\partial(J\Gamma_\Phi g^{22}\dfrac{\partial\Phi}{\partial x^2})}{\partial x^2} + S_i'(x^1, x^2) \quad (7)$$

The physical contravariant velocity components, V^1, V^2 are defined as:

$$V^1 = J(v_x\partial x^1/\partial x + v_y\partial x^1/\partial y), \quad V^2 = J(v_x\partial x^2/\partial x + v_y\partial x^2/\partial y), \quad (8)$$

where J is Jacobian of coordinate transformation.

The source term can be written as:

$$S_i'(x^1, x^2) = JS_\Phi + \partial(J\Gamma_\Phi g^{12}\partial\Phi/\partial x^2)/\partial x^1 + \partial(J\Gamma_\Phi g^{21}\partial\Phi/\partial x^3)/\partial x^2 \quad (9)$$

The discretized algebraic equations of generalized Eq.(7) are solved by using the pressure correction method. A central volume approximation is used for all diffusion terms, and an up-winding scheme is used for convection terms. All difference equations can be written in a generalized version. A staggered grid arrangement is used in this method for stable solution. The solution procedure is the same as the SIMPLE method (please see Launder and Spalding and Patankar's papers). Then, the static pressure is corrected for each iteration.

CALCULATION EXAMPLE

In this paper a two-dimensional steady tapping flow field was calculated. The Reynolds number based on the pipe diameter and velocity is 87,300.

The upper figure of Figure 1 shows the principle scheme of the flow field. In the actual cell there are two layers of liquid, bath and metal. In our case the fluid flow is assumed to be a single phase and uniform. The liquid height and the clearance height (i.e. the distance from the tapping pipe to the cathode surface) are denoted by *B* and *Hcl*, respectively. The leaning angle between the tapping pipe and the bath level is denoted by σ. In this figure σ is equal to *60* degrees. Since the intensity of cathode erosion is proportional to the surface stress and velocity in the entrance region on the cathode bottom, the greater the intensity of the surface stress, the faster is the erosion of the cathode. The influence of the leaning angle, σ, and the clearance ratio, *Hcl/B*, on the surface stress is an important problem in the present study.

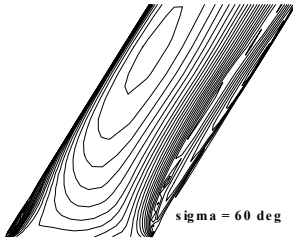

Figure 3. Velocity contours in the pipe.

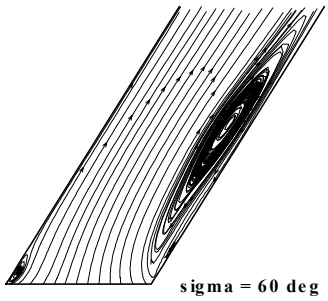

Figure 4. Vortices by particle traces in the pipe.

In the lower figure of Figure 1 a body-fitted grid system is plotted. As shown in the figure a non-uniform grid system is used. The meshes near walls and pipe inlet are finer. From calculations it is known that there is no need of calculation for the full flow field. The flow field inside pipe with the clearance is calculated in this paper. The following boundary conditions are adopted: (1) at the bottom and pipe walls no-slip condition is taken, i.e.

velocity at wall equals zero; (2) at inlet to the clearance zone the total pressure is given; (3) at outlet from the tapping pipe the static pressure is also given and the gradient of static pressure and velocity are taken to be zero. The calculations for different leaning angles and different clearance heights were carried on.

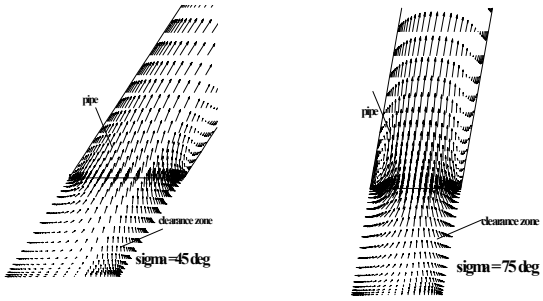

Figure 5. Vector schemes inside pipe and clearance.

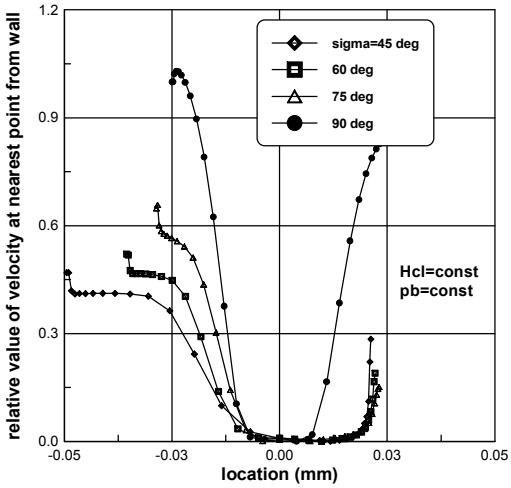

Figure 6. Distributions of relative values of velocity at nearest grid point.

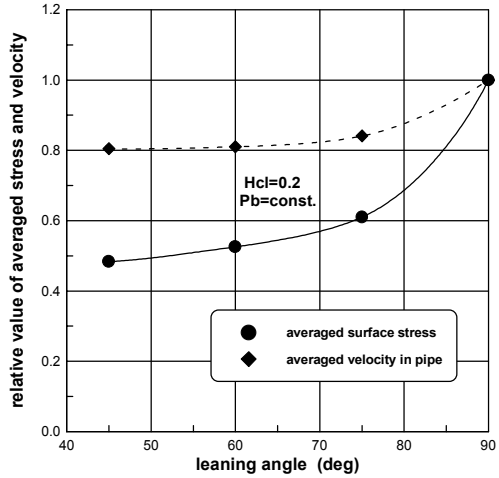

Figure7. Averaged stress and velocity in pipe via leaning angle.

Velocity vector schemes inside pipe and clearance for different leaning angles

In this section we will show you the clearance and the leaning angle of the tapping pipe are two important parameters of tapping problem. Understanding the their effects on the erosion intensity enables us to improve the tapping process. In Figure 2 the velocity vector schemes inside pipe and clearance zone are demonstrated. The results are for the leaning angle of 60 degrees. The left figure of Figure 2 shows the enlarged velocity schemes in the clearance zone. It is seen that the fluid comes from left and right sides into the clearance zone. In Figure 3 the velocity contours are plotted. On both walls of the pipe the flow is separated. As shown in Figure 4, the vortex near the right wall is much stronger than the vortex near the left wall. In Figure 5 the velocity vector schemes for leaning angles of 45 and 75 degrees are also plotted. From the figure it can be found that the intensity of the left wall vortex is increased with increasing the leaning angle.

Effect of leaning angle on surface stress

It is known that the surface stress can be expressed as follows:

$$\tau = \mu \, dV / dn$$

and the velocity gradient can be expressed by the following approximate formula:

$$dV / dn \cong (V_{+1} - 0) / \Delta n$$

where, V_{+1} denotes the velocity at the nearest grid point from the bottom wall; Δn is the distance of the nearest grid point from the bottom wall. Therefore, the erosion intensity is proportional to the velocity at the nearest grid point from the bottom wall. In Figure 6 the distributions of the relative values of the velocity at the nearest grid point from wall for different leaning angles, $V / V_{\sigma=90}$, are plotted. As shown in the figure, the greater the leaning angle, the greater is the velocity, and then the intensity of the surface stress is greater. This feature can be found from Figure 7. The definition of the relative value of averaged stress is the ratio of (bottom surface) area-averaged stress to the area-averaged stress of leaning angle of *90* degrees. The mass-averaged velocity in the tapping pipe is also plotted in the same figure. It is seen that the flow rate past the tapping pipe is increased with increasing the leaning angle. For the case of constant clearance there exists a compromise between erosion and productivity.

Effect of clearance on surface stress

For the leaning angle of 60 degrees the tapping flows of four clearance/bath-metal height ratios were calculated. They are *Hcl/B= 0.10, 0.15, 0.20, 0.25* and *0.30*. From Figure 8 we can see that the averaged surface stress of the clearance bottom area is decreased with the increase of the clearance/bath-metal height ratio. We can not choose very large clearance/bath-metal height ratios. This is for avoidance of bath entrainment. The upper limit of the clearance/bath-metal height ratio is defined by the case when no bath entrainment is happened (Walker, 1997). This phenomenon can not be observed by two-dimensional simulation. Therefore, to develop a three-dimensional computational method for tapping flow study is very important.

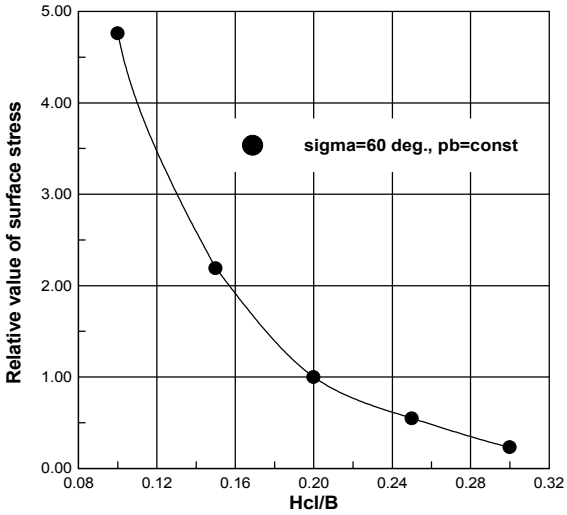

Figure 8. Surface stress via relative value of clearance.

Figure 9 shows the relative value of averaged surface stress via velocity in pipe. In this case the back static pressure and the leaning angle remain constant. From this figure it is seen that surface stress is a function of the clearance value.

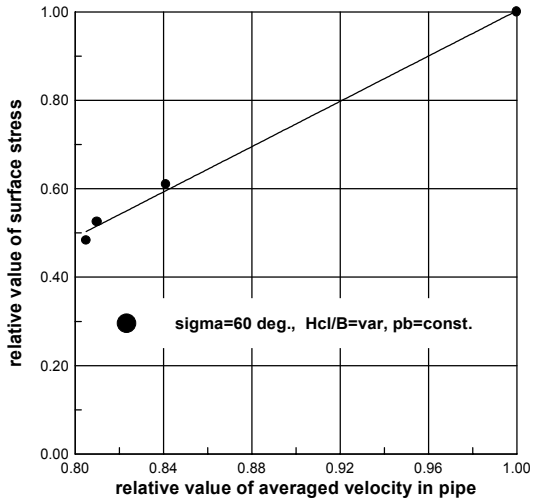

Figure 9. Relative value of averaged surface stress via velocity in pipe.

CONCLUSIONS

From practice we know the phenomenon of cathode erosion is a mass transfer process. Apparently, the intensity of mass transfer is a function of surface stress, or drag force acting at per area. Therefore, we can use the surface stress at the entrance region on the cathode bottom to characterize the intensity of the cathode erosion approximately. Then, the intensity of cathode erosion is proportional to the surface stress in the entrance region on the cathode bottom, the greater the intensity of the surface stress, the faster is the erosion of the cathode. In the present paper a pressure correction method using Navier-Stokes solver is presented to study liquid aluminum metal tapping flows. At beginning of the paper the basic equations of the two-dimensional turbulent flow are given. The equations are written in a generalized form for adapting the body-fitted coordinate system. Then, a 2-D steady tapping flow is calculated and studied. The flow fields for different leaning angles with constant Hcl / B of 0.2 and for different clearance/bath-metal height ratios with constant leaning angle of *60* degrees are calculated. The calculated results show that the surface stress on the clearance bottom is increased with the increase of leaning angle and decreased with the increase of clearance/bath-metal height ratio. The calculations also show that the averaged surface stress on the cathode bottom is a function of the averaged velocity inside tapping pipe. The further studies of detail mechanism of the flows at different tapping regimes and the effect of the tapping spout geometry require developing a three-dimensional simulation method.

ACKNOWLEDGEMENTS

The authors would like to acknowledge China National Natural Science Foundation and the New Zealand Foundation for Research Science and Technology for their partial support to this work.

REFERENCE

CHEN, Naixing and XU, Yanji (1990) Numerical Computation of 3-D Turbulent Flow in Turbine Cascade, Chinese Sciences Bulletin, Vol. 35, No. 14.

CHEN, Naixing and XU, Yanji (1991) Numerical Solution of 2D and 3D Turbulent Internal Flow Problems, Int. J. Of Numerical Methods in Fluid, Vol. 13, No. 2.

LAUNDER, B. E. and SPALDING, D. B. (1974) The Numerical Computation of Turbulent Flows, Computational Methods In Applied Mechanical Engineering, Vol. 3, pp.269-289.Patankar, S. V. (1980) Numerical Transfer and Fluid Flow, McGraw Hill, New York.

WALKER, Marcus L. (1997) Visualization of Tapping Flows, Light Metals 1997, Edited by Reidar Huglen, The Minerals, Metals and Materials Society.